In collaboration with:

Orlando Panella, INFN Perugia
C. Carimalo and W. Da Silva (LPNHE, Paris VI)

SUSY Lepton flavor Violation at Photon Colliders

hep/ph 0508256, LPNHE 2005-11, Phys. Rev. D **72**, 115004 (2005)

Mirco Cannoni

Università di Perugia
INFN Sezione di Perugia

Frascati, May 18, 2006
LNF Spring School

1. Introduction

Outline

Motivations

- Neutrino masses $\neq 0$ hint to lepton flavour violation (LFV) $\ell \to \ell' + \gamma$. However in the standard Model (SM) such processes are strongly suppressed: $Br \approx \mathcal{O}(10^{-40})$

Motivations

- Neutrino masses $\neq 0$ hint to lepton flavour violation (LFV) $\ell \to \ell' + \gamma$. However in the standard Model (SM) such processes are strongly suppressed: $Br \approx \mathcal{O}(10^{-40})$
- $Br(\mu \to e\gamma) < 1.2 \times 10^{-11}$ [MEGA, PRD 65 2002 112002]
  $Br(\tau \to e\gamma) < 3.9 \times 10^{-7}$ [BELLE hep-ex/0501068]
  $Br(\tau \to \mu\gamma) < 6.8 \times 10^{-8}$ [BABAR hep-ex 0502032, PRL 92 171802].

Motivations

- Neutrino masses $\neq 0$ hint to lepton flavour violation (LFV) $\ell \to \ell' + \gamma$. However in the standard Model (SM) such processes are strongly suppressed: $Br \approx \mathcal{O}(10^{-40})$
- $Br(\mu \to e\gamma) < 1.2 \times 10^{-11}$ [MEGA, PRD 65 2002 112002]
  $Br(\tau \to e\gamma) < 3.9 \times 10^{-7}$ [BELLE hep-ex/0501068]
  $Br(\tau \to \mu\gamma) < 6.8 \times 10^{-8}$ [BABAR hep-ex 0502032, PRL 92 171802].
- New Physics is needed to have rates which would be detectable. The SUSY see-saw mechanism provides sources of LFV potentially observable

Motivations

- Neutrino masses $\neq 0$ hint to lepton flavour violation (LFV) $\ell \rightarrow \ell' + \gamma$. However in the standard Model (SM) such processes are strongly suppressed: $Br \approx \mathcal{O}(10^{-40})$
- $Br(\mu \rightarrow e\gamma) < 1.2 \times 10^{-11}$ [MEGA, PRD 65 2002 112002]
  $Br(\tau \rightarrow e\gamma) < 3.9 \times 10^{-7}$ [BELLE hep-ex/0501068]
  $Br(\tau \rightarrow \mu\gamma) < 6.8 \times 10^{-8}$ [BABAR hep-ex 0502032, PRL 92 171802].
- New Physics is needed to have rates which would be detectable. The SUSY see-saw mechanism provides sources of LFV potentially observable
- Extend to the $\gamma\gamma$ option a previous analysis by some of the authors for the $e^+e^- \rightarrow \ell\ell'$ and $e^-e^- \rightarrow \ell\ell'$ processes at a Linear Collider. [M. Cannoni, S. Kolb and O. Panella, Phys. Rev. D **68**, 096002 (2003) arXiv:hep-ph/0306170]

Motivations

- Neutrino masses $\neq 0$ hint to lepton flavour violation (LFV) $\ell \to \ell' + \gamma$. However in the standard Model (SM) such processes are strongly suppressed: $Br \approx \mathcal{O}(10^{-40})$
- $Br(\mu \to e\gamma) < 1.2 \times 10^{-11}$ [MEGA, PRD 65 2002 112002]
  $Br(\tau \to e\gamma) < 3.9 \times 10^{-7}$ [BELLE hep-ex/0501068]
  $Br(\tau \to \mu\gamma) < 6.8 \times 10^{-8}$ [BABAR hep-ex 0502032, PRL 92 171802].
- New Physics is needed to have rates which would be detectable. The SUSY see-saw mechanism provides sources of LFV potentially observable
- Extend to the $\gamma\gamma$ option a previous analysis by some of the authors for the $e^+e^- \to \ell\ell'$ and $e^-e^- \to \ell\ell'$ processes at a Linear Collider. [M. Cannoni, S. Kolb and O. Panella, Phys. Rev. D **68**, 096002 (2003) arXiv:hep-ph/0306170]
- Study the lepton flavor violating reaction $\gamma\gamma \to \ell\ell'$ with $\ell \neq \ell'$ and $\ell, \ell' = e, \mu, \tau$, (one loop order) in the SUSY see-saw scenario, at a Photon Collider.

Signal features

- $\gamma\gamma \to \ell\ell'$ has the advantage of providing a clean final state which is easy to identify experimentally (two back to back different flavor leptons), though one has to pay the price of dealing with cross sections of order $\mathcal{O}(\alpha^4)$.

Signal features

- $\gamma\gamma \to \ell\ell'$ has the advantage of providing a clean final state which is easy to identify experimentally (two back to back different flavor leptons), though one has to pay the price of dealing with cross sections of order $\mathcal{O}(\alpha^4)$.
- In general the $\gamma\gamma$ mode offers larger cross section respect to the other modes (e^+e^- and e^-e^-).

Signal features

- $\gamma\gamma \to \ell\ell'$ has the advantage of providing a clean final state which is easy to identify experimentally (two back to back different flavor leptons), though one has to pay the price of dealing with cross sections of order $\mathcal{O}(\alpha^4)$.
- In general the $\gamma\gamma$ mode offers larger cross section respect to the other modes (e^+e^- and e^-e^-).
- However larger background are expected

Signal features

- $\gamma\gamma \to \ell\ell'$ has the advantage of providing a clean final state which is easy to identify experimentally (two back to back different flavor leptons), though one has to pay the price of dealing with cross sections of order $\mathcal{O}(\alpha^4)$.
- In general the $\gamma\gamma$ mode offers larger cross section respect to the other modes (e^+e^- and e^-e^-).
- However larger background are expected
- In addition non-monochromaticity of the beams must be taken into account.

Outline

SUSY see-saw mechanism

- The superpotential W contains three $SU(2)_L$ singlet neutrino superfields N_i with the following couplings:

$$W = (Y_\nu)_{ij}\varepsilon_{\alpha\beta}H_2^\alpha N_i L_j^\beta + \frac{1}{2}(M_R)_i N_i N_i.$$

H_2 is a Higgs doublet superfield, L_i are the $SU(2)_L$ doublet lepton superfields, Y_ν is a Yukawa coupling matrix and M_R is the $SU(2)_L$ singlet neutrino mass matrix.

SUSY see-saw mechanism

- The superpotential W contains three $SU(2)_L$ singlet neutrino superfields N_i with the following couplings:

$$W = (Y_\nu)_{ij}\varepsilon_{\alpha\beta}H_2^\alpha N_i L_j^\beta + \frac{1}{2}(M_R)_i N_i N_i.$$

H_2 is a Higgs doublet superfield, L_i are the $SU(2)_L$ doublet lepton superfields, Y_ν is a Yukawa coupling matrix and M_R is the $SU(2)_L$ singlet neutrino mass matrix.

- With the additional Yukawa couplings and the new mass scale (M_R) the RGE evolution from the GUT scale down to M_R induce *off-diagonal* matrix elements in charged sleptons mass matrix $(m^2_{\tilde{L}})_{ij}$.

One Loop result

- In the one loop approximation the off-diagonal elements of the charged sleptons mass matrix are [Borzumati-Masiero, Hisano et al.]:

$$(m^2_{\tilde{L}})_{ij} \simeq -\frac{1}{8\pi^2}(3+a_0^2)m_0^2(Y_\nu^\dagger Y_\nu)_{ij} \ln\left(\frac{M_{GUT}}{M_R}\right).$$

where a_0 is a dimensionless parameter appearing in the matrix of trilinear mass terms $A_\ell = Y_\ell a_0 m_0$ contained in V_{soft}.

One Loop result

- In the one loop approximation the off-diagonal elements of the charged sleptons mass matrix are [Borzumati-Masiero, Hisano et al.]:

$$(m^2_{\tilde{L}})_{ij} \simeq -\frac{1}{8\pi^2}(3+a_0^2)m_0^2(Y_\nu^\dagger Y_\nu)_{ij}\ln\left(\frac{M_{GUT}}{M_R}\right).$$

  where a_0 is a dimensionless parameter appearing in the matrix of trilinear mass terms $A_\ell = Y_\ell a_0 m_0$ contained in V_{soft}.

- These off diagonal matrix elements can be potentially large because they are not directly related to the mass of the light neutrinos, but only through the seesaw relation $m_\nu \simeq m_D^2/M_R = v^2 Y_\nu^2/M_R$.

Two generation model

- Assume for the mass matrix of the charged left-sleptons (and sneutrinos):

$$\widetilde{m}_L^2 = \begin{pmatrix} \widetilde{m}^2 & \Delta m^2 \\ \Delta m^2 & \widetilde{m}^2 \end{pmatrix},$$

with eigenvalues: $\widetilde{m}_\pm^2 = \widetilde{m}^2 \pm \Delta m^2$ and maximal mixing.

Two generation model

- Assume for the mass matrix of the charged left-sleptons (and sneutrinos):

$$\widetilde{m}_L^2 = \begin{pmatrix} \widetilde{m}^2 & \Delta m^2 \\ \Delta m^2 & \widetilde{m}^2 \end{pmatrix},$$

with eigenvalues: $\widetilde{m}_\pm^2 = \widetilde{m}^2 \pm \Delta m^2$ and maximal mixing.

- After diagonalization of the mass matrix the LFV propagator for a scalar line is

$$\langle \tilde{\ell}_i \tilde{\ell}_j^\dagger \rangle_0 = \frac{i}{2}\left(\frac{1}{p^2 - \widetilde{m}_+^2} - \frac{1}{p^2 - \widetilde{m}_-^2}\right) = i\frac{\Delta m^2}{(p^2 - \widetilde{m}_+^2)(p^2 - \widetilde{m}_-^2)}$$

Two generation model

- Assume for the mass matrix of the charged left-sleptons (and sneutrinos):

$$\widetilde{m}_L^2 = \begin{pmatrix} \widetilde{m}^2 & \Delta m^2 \\ \Delta m^2 & \widetilde{m}^2 \end{pmatrix},$$

with eigenvalues: $\widetilde{m}_\pm^2 = \widetilde{m}^2 \pm \Delta m^2$ and maximal mixing.

- After diagonalization of the mass matrix the LFV propagator for a scalar line is

$$\langle \tilde{\ell}_i \tilde{\ell}_j^\dagger \rangle_0 = \frac{i}{2}\left(\frac{1}{p^2 - \widetilde{m}_+^2} - \frac{1}{p^2 - \widetilde{m}_-^2} \right) = i \frac{\Delta m^2}{(p^2 - \widetilde{m}_+^2)(p^2 - \widetilde{m}_-^2)}$$

- The quantity $\delta_{LL} = \Delta m^2 / \widetilde{m}^2$ is the dimension-less parameter that controls the magnitude of the LFV effect.

Two generation model

- Assume for the mass matrix of the charged left-sleptons (and sneutrinos):
$$\widetilde{m}_L^2 = \begin{pmatrix} \widetilde{m}^2 & \Delta m^2 \\ \Delta m^2 & \widetilde{m}^2 \end{pmatrix},$$
with eigenvalues: $\widetilde{m}_\pm^2 = \widetilde{m}^2 \pm \Delta m^2$ and maximal mixing.
- After diagonalization of the mass matrix the LFV propagator for a scalar line is
$$\langle \tilde{\ell}_i \tilde{\ell}_j^\dagger \rangle_0 = \frac{i}{2}\left(\frac{1}{p^2 - \widetilde{m}_+^2} - \frac{1}{p^2 - \widetilde{m}_-^2}\right) = i \frac{\Delta m^2}{(p^2 - \widetilde{m}_+^2)(p^2 - \widetilde{m}_-^2)}$$
- The quantity $\delta_{LL} = \Delta m^2 / \widetilde{m}^2$ is the dimension-less parameter that controls the magnitude of the LFV effect.
- Our propagator corresponds to the one in the Mass Insertion Approximation when one assumes equal diagonal masses squred (good at the electroweak scale due to degeneracy) and $\Delta m^2 \ll \widetilde{m}^2$ which is necessary for the expansion in powers of δ_{LL}.

Two generation model

- This approach allows us to study the signal in a quite model-independent way by means of scans in the parameter space – the $\widetilde{m}, \delta_{LL}$ plane – which is already constrained by the experimental bounds of radiative lepton decay processes.

Two generation model

- This approach allows us to study the signal in a quite model-independent way by means of scans in the parameter space – the $\widetilde{m}, \delta_{LL}$ plane – which is already constrained by the experimental bounds of radiative lepton decay processes.
- assume that the two lightest neutralinos are pure Bino and pure Wino with masses M_1 and M_2 respectively, while charginos are pure charged Winos with mass M_2, M_1 and M_2 being the gaugino masses in the soft breaking potential.

Two generation model

- This approach allows us to study the signal in a quite model-independent way by means of scans in the parameter space – the $\widetilde{m}, \delta_{LL}$ plane – which is already constrained by the experimental bounds of radiative lepton decay processes.
- assume that the two lightest neutralinos are pure Bino and pure Wino with masses M_1 and M_2 respectively, while charginos are pure charged Winos with mass M_2, M_1 and M_2 being the gaugino masses in the soft breaking potential.
- The Higgsino contribution to neutralino and charginos is suppressed, since the coupling is proportional to the lepton masses and so their contribution is neglected.

Two generation model

- This approach allows us to study the signal in a quite model-independent way by means of scans in the parameter space – the $\widetilde{m}, \delta_{LL}$ plane – which is already constrained by the experimental bounds of radiative lepton decay processes.
- assume that the two lightest neutralinos are pure Bino and pure Wino with masses M_1 and M_2 respectively, while charginos are pure charged Winos with mass M_2, M_1 and M_2 being the gaugino masses in the soft breaking potential.
- The Higgsino contribution to neutralino and charginos is suppressed, since the coupling is proportional to the lepton masses and so their contribution is neglected.
- Under these assumptions the signal cross section does not depend on $\tan\beta$ while for radiative decays gaugino-higgsino contributions are dominant ($\tan\beta$ enhanced) and considered by diagonalization of all the mass matrices

Contributing diagrams to $\gamma\gamma \to \ell\ell'$

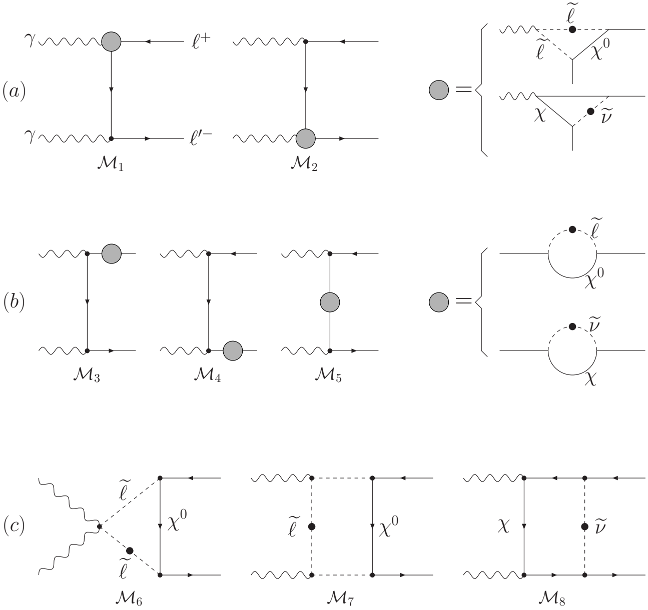

- (a) Penguin

Contributing diagrams to $\gamma\gamma \to \ell\ell'$

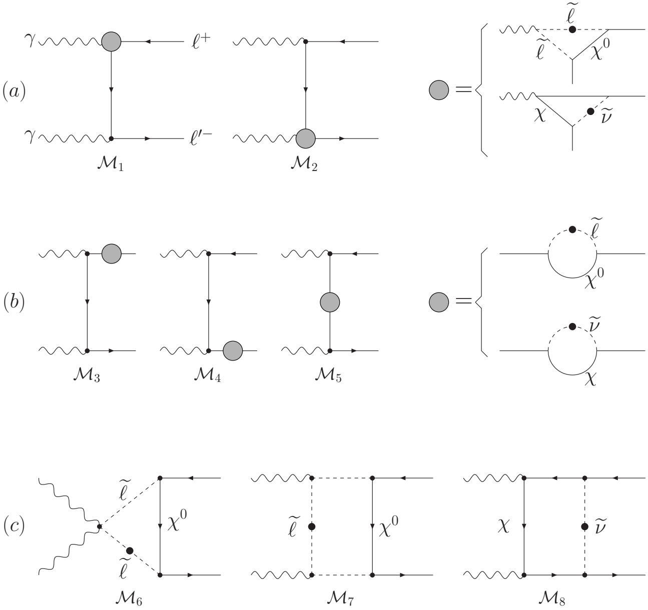

- (a) Penguin
- (b) Self-energy

Contributing diagrams to $\gamma\gamma \to \ell\ell'$

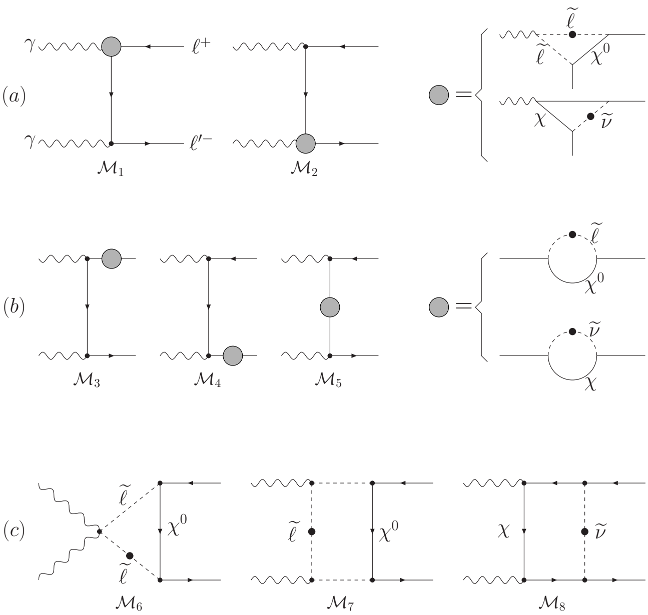

- (a) Penguin
- (b) Self-energy
- (c) Box diagrams

Contributing diagrams to $\gamma\gamma \to \ell\ell'$

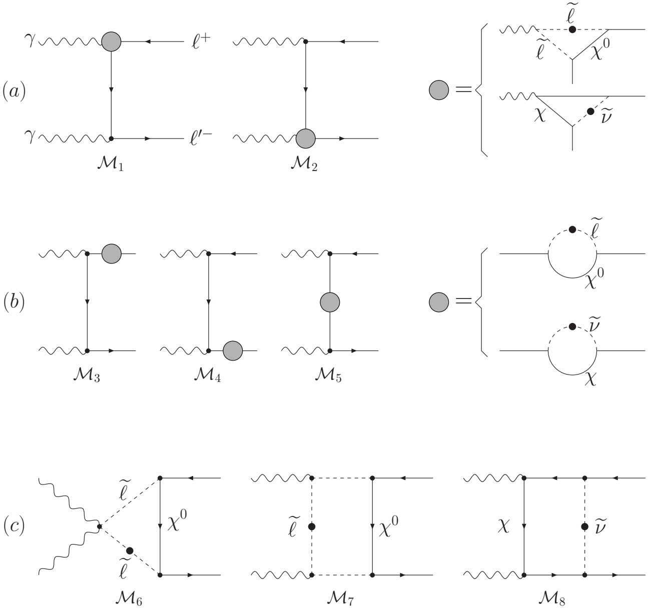

- (a) Penguin
- (b) Self-energy
- (c) Box diagrams
- The full black circle stands for a LFV propagator

Contributing diagrams to $\gamma\gamma \to \ell\ell'$

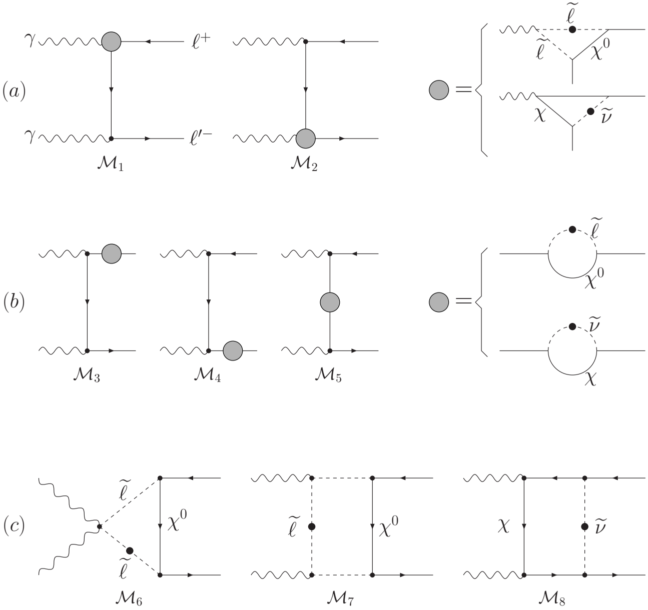

- (a) Penguin
- (b) Self-energy
- (c) Box diagrams
- The full black circle stands for a LFV propagator
- Every diagrams is accompained by an exchange graph.

Helicity Amplitudes for $\gamma\gamma \to \ell\ell'$

- Assume massless external fermions. The chiral nature of the coupling in the $\mathcal{L}_{int}$, fixes the helicity of the fermions in the final to only one configuration: *thus there are only four helicity amplitudes corresponding to the possible combinations of the photon helicities.*

Helicity Amplitudes for $\gamma\gamma \to \ell\ell'$

- Assume massless external fermions. The chiral nature of the coupling in the $\mathcal{L}_{int}$, fixes the helicity of the fermions in the final to only one configuration: *thus there are only four helicity amplitudes corresponding to the possible combinations of the photon helicities.*
- Let $\mathcal{M}^{(\lambda,\lambda')}$ the helicity amplitudes: $\mathcal{M}^{(+,+)}$, $\mathcal{M}^{(+,-)}$, $\mathcal{M}^{(-,+)}$, $\mathcal{M}^{(-,-)}$.

Helicity Amplitudes for $\gamma\gamma \to \ell\ell'$

- Assume massless external fermions. The chiral nature of the coupling in the $\mathcal{L}_{int}$, fixes the helicity of the fermions in the final to only one configuration: *thus there are only four helicity amplitudes corresponding to the possible combinations of the photon helicities.*
- Let $\mathcal{M}^{(\lambda,\lambda')}$ the helicity amplitudes: $\mathcal{M}^{(+,+)}$, $\mathcal{M}^{(+,-)}$, $\mathcal{M}^{(-,+)}$, $\mathcal{M}^{(-,-)}$.
- The final analytical formulas of the amplitudes $\mathcal{M}^{(\lambda,\lambda')}$ are function of s, θ^*, λ, λ', $\widetilde{m}$, δ_{LL} and the form factors for the loop integrals.

$$\mathcal{M}^{(\lambda,\lambda')} = (s, \theta^*, \lambda, \lambda', \widetilde{m}, \delta_{LL})$$

Outline

High Energy photon collisions

- High energy photons beams will be obtained from Compton back-scattered (CB) low energy laser photons with energy ω_0 off high energy electron beams with energy E_0.

Ginzburg, Kotkin, Serbo and Telnov, NIM **205** 47 (1983);
Ginzburg, Kotkin, Panfil, Serbo and Telnov, NIM 219 5 (1984).
Badelek *et al.* [ECFA/DESY Photon Collider Working Group], Int. J. Mod. Phys. A **19**, 5097 (2004), [arXiv:hep-ex/0108012]
Web page on TDR Photon Collider:
http://www.desy.de./ telnov/tdr/ggtdr.ps.gz

High Energy photon collisions

- High energy photons beams will be obtained from Compton back-scattered (CB) low energy laser photons with energy ω_0 off high energy electron beams with energy E_0.
- High energy photon beams *will not be* monochromatic but *will present* instead an energy spectrum, mainly determined by the Compton cross section, up to a maximum energy $y_m E_0$, where $y_m = x/(x+1)$ with $x = 4E_0\omega_0/m_e^2$.

Ginzburg, Kotkin, Serbo and Telnov, NIM **205** 47 (1983);
Ginzburg, Kotkin, Panfil, Serbo and Telnov, NIM 219 5 (1984).
Badelek *et al.* [ECFA/DESY Photon Collider Working Group], Int. J. Mod. Phys. A **19**, 5097 (2004), [arXiv:hep-ex/0108012]
Web page on TDR Photon Collider:
http://www.desy.de./ telnov/tdr/ggtdr.ps.gz

High Energy photon collisions

- High energy photons beams will be obtained from Compton back-scattered (CB) low energy laser photons with energy ω_0 off high energy electron beams with energy E_0.
- High energy photon beams *will not be* monochromatic but *will present* instead an energy spectrum, mainly determined by the Compton cross section, up to a maximum energy $y_m E_0$, where $y_m = x/(x+1)$ with $x = 4E_0\omega_0/m_e^2$.
- Full simulations show that there will be also a low energy broad peak (multiple Compton scattering and beamstrahlung)

Ginzburg, Kotkin, Serbo and Telnov, NIM **205** 47 (1983);
Ginzburg, Kotkin, Panfil, Serbo and Telnov, NIM 219 5 (1984).
Badelek *et al.* [ECFA/DESY Photon Collider Working Group], Int. J. Mod. Phys. A **19**, 5097 (2004), [arXiv:hep-ex/0108012]
Web page on TDR Photon Collider:
http://www.desy.de./ telnov/tdr/ggtdr.ps.gz

High Energy photon collisions

- High energy photons beams will be obtained from Compton back-scattered (CB) low energy laser photons with energy ω_0 off high energy electron beams with energy E_0.
- High energy photon beams *will not be* monochromatic but *will present* instead an energy spectrum, mainly determined by the Compton cross section, up to a maximum energy $y_m E_0$, where $y_m = x/(x+1)$ with $x = 4E_0\omega_0/m_e^2$.
- Full simulations show that there will be also a low energy broad peak (multiple Compton scattering and beamstrahlung)
- However the high energy peak is well described by the analytical Compton spectrum

Ginzburg, Kotkin, Serbo and Telnov, NIM **205** 47 (1983);
Ginzburg, Kotkin, Panfil, Serbo and Telnov, NIM 219 5 (1984).
Badelek *et al.* [ECFA/DESY Photon Collider Working Group], Int. J. Mod. Phys. A **19**, 5097 (2004), [arXiv:hep-ex/0108012]
Web page on TDR Photon Collider:
http://www.desy.de./ telnov/tdr/ggtdr.ps.gz

Differential CB luminosity

The high energy peak is almost independent from technological details and ≈ by the product of two CB spectra ($y_{1,2} = E_{\gamma_{1,2}/E_0}$):

$$\frac{dL_{\gamma\gamma}^{CB}}{dy_1\, dy_2} = F_c(x, y_1)\, F_c(x, y_2)$$

Differential CB luminosity

The high energy peak is almost independent from technological details and ≈ by the product of two CB spectra ($y_{1,2} = E_{\gamma_{1,2}/E_0}$):

$$\frac{dL_{\gamma\gamma}^{CB}}{dy_1\, dy_2} = F_c(x, y_1)\, F_c(x, y_2)$$

The theoretical differential luminosity spectrum is:

$$\frac{dL_{\gamma\gamma}^{CB}}{dz} = 2z \int_{-\ln \frac{y_m}{z}}^{\ln \frac{y_m}{z}} d\eta F_c(x, ze^{+\eta}) F_c(x, ze^{-\eta})$$

($z = \sqrt{y_1 y_2} = W_{\gamma\gamma}/2E_0 = \sqrt{s_{\gamma\gamma}/s_{ee}}$ and the "*pseudorapidity*" $\eta = \ln \sqrt{y_1/y_2}$)

Differential CB luminosity

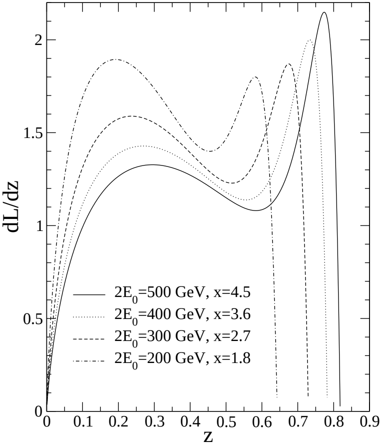

The high energy peak is almost independent from technological details and ≈ by the product of two CB spectra ($y_{1,2} = E_{\gamma_{1,2}/E_0}$):

$$\frac{dL^{CB}_{\gamma\gamma}}{dy_1\,dy_2} = F_c(x, y_1)\,F_c(x, y_2)$$

The theoretical differential luminosity spectrum is:

$$\frac{dL^{CB}_{\gamma\gamma}}{dz} = 2z\int_{-\ln\frac{y_m}{z}}^{\ln\frac{y_m}{z}} d\eta F_c(x, ze^{+\eta})F_c(x, ze^{-\eta})$$

($z = \sqrt{y_1\,y_2} = W_{\gamma\gamma}/2E_0 = \sqrt{s_{\gamma\gamma}/s_{ee}}$ and the "*pseudorapidity*" $\eta = \ln\sqrt{y_1/y_2}$)

Normalization of Luminosity spectrum

- Simulated values of luminosities $L_{\gamma\gamma}$ at the peak: $L_{\gamma\gamma}(z > 0.8 z_m)$ [Telnov] :

$\sqrt{s_{ee}} = 2E_0$	L_0 10^{34} cm^{-2} s^{-1}	$L_{\gamma\gamma}$ 10^{34} cm^{-2} s^{-1}	$L_{\gamma\gamma}$ fb^{-1}yr^{-1}
200 GeV	4.8	19.1	130
500 GeV	0.44	1.15	340

- Normalization condition:

$$L_{\gamma\gamma}(z > z_{max}) = \int_{0.8 z_{max}}^{z_{max}} dz \frac{dL_{\gamma\gamma}}{dz}$$

Normalization of Luminosity spectrum

- Simulated values of luminosities $L_{\gamma\gamma}$ at the peak: $L_{\gamma\gamma}(z > 0.8 z_m)$ [Telnov] :

$\sqrt{s_{ee}} = 2E_0$	L_0 10^{34} cm^{-2} s^{-1}	$L_{\gamma\gamma}$ 10^{34} cm^{-2} s^{-1}	$L_{\gamma\gamma}$ fb^{-1}yr^{-1}
200 GeV	4.8	19.1	130
500 GeV	0.44	1.15	340

- Normalization condition:

$$L_{\gamma\gamma}(z > z_{max}) = \int_{0.8 z_{max}}^{z_{max}} dz \frac{dL_{\gamma\gamma}}{dz}$$

- Define both for signal and background the *effective* cross section to be:

$$\sigma^{effective} = \int_{z_{min}}^{z_{max}} dz \frac{dL_{\gamma\gamma}^{norm}}{dz} \sigma(W_{\gamma\gamma})$$

Normalization of Luminosity spectrum

- Simulated values of luminosities $L_{\gamma\gamma}$ at the peak: $L_{\gamma\gamma}(z > 0.8 z_m)$ [Telnov] :

$\sqrt{s_{ee}} = 2E_0$	L_0 10^{34} cm^{-2} s^{-1}	$L_{\gamma\gamma}$ 10^{34} cm^{-2} s^{-1}	$L_{\gamma\gamma}$ fb^{-1}yr^{-1}
200 GeV	4.8	19.1	130
500 GeV	0.44	1.15	340

- Normalization condition:

$$L_{\gamma\gamma}(z > z_{max}) = \int_{0.8 z_{max}}^{z_{max}} dz \frac{dL_{\gamma\gamma}}{dz}$$

- Define both for signal and background the *effective* cross section to be:

$$\sigma^{effective} = \int_{z_{min}}^{z_{max}} dz \frac{dL^{norm}_{\gamma\gamma}}{dz} \sigma(W_{\gamma\gamma})$$

- The total number of events is given by

$$N_{events} = L_{\gamma\gamma} \times \sigma^{effective}$$

Ideal CB helicity spectrum

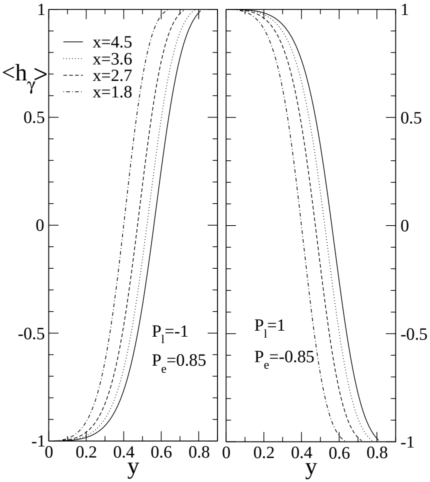

- Photons also show an helicity spectrum.

Ideal CB helicity spectrum

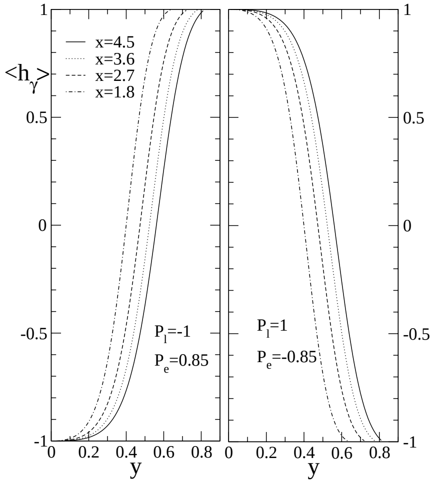

- Photons also show an helicity spectrum.
- in the high energy peak ($y \approx y_m$) photons have a high degree of circular polarization $P_\gamma = -P_\ell = P_{laser}$

Signal cross sections

- The differential cross sections as a function the scattering angle in the photon-photon CMF (case of monochromatic and polarized photons) are given by:

$$\frac{d\hat{\sigma}^{\lambda\lambda'}}{d\cos\theta^*} = \frac{1}{32\pi\hat{s}}\left|\mathcal{M}^{\lambda\lambda'}(\hat{s},\hat{t},\hat{u},\widetilde{m},\delta_{LL})\right|^2,$$

Signal cross sections

- The differential cross sections as a function the scattering angle in the photon-photon CMF (case of monochromatic and polarized photons) are given by:

$$\frac{d\hat{\sigma}^{\lambda\lambda'}}{d\cos\theta^*} = \frac{1}{32\pi\hat{s}}\left|\mathcal{M}^{\lambda\lambda'}(\hat{s},\hat{t},\hat{u},\widetilde{m},\delta_{LL})\right|^2,$$

- The realistic effective differential cross sections as a function scattering angle in the laboratory system (e^-e^- center of mass system) are obtained by boosting to the lab-system with the luminosity spectrum

$$\frac{d\sigma^{\lambda\lambda'}}{d\cos\theta} = \int_{z_{min}}^{z_{max}} dz\,\frac{dL_{\gamma\gamma}^{norm}}{dz}|J|\frac{(1-\langle\lambda\rangle)}{2}\frac{(1-\langle\lambda'\rangle)}{2}\frac{d\hat{\sigma}^{\lambda\lambda'}}{d\cos\theta^*}$$

Monochromatic angular distributions

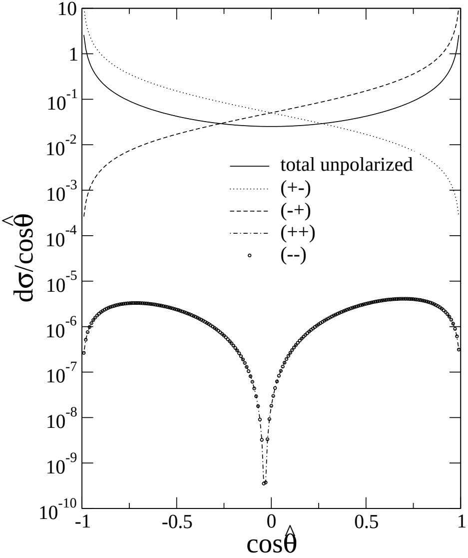

- $\mathcal{M}^{(+,-)}$ peaked in the backward direction $\mathcal{M}^{(-,+)}$ peaked in the forward direction $(J_z = \pm 2)$

Monochromatic angular distributions

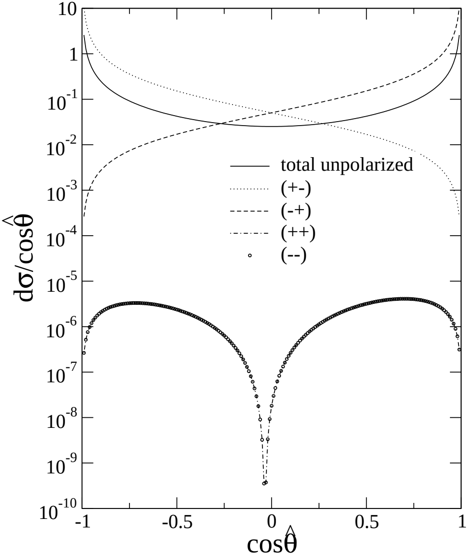

- $\mathcal{M}^{(+,-)}$ peaked in the backward direction $\mathcal{M}^{(-,+)}$ peaked in the forward direction ($J_z = \pm 2$)
- Dominance of diagrams with exchange of a massless lepton in t and u channel

Monochromatic angular distributions

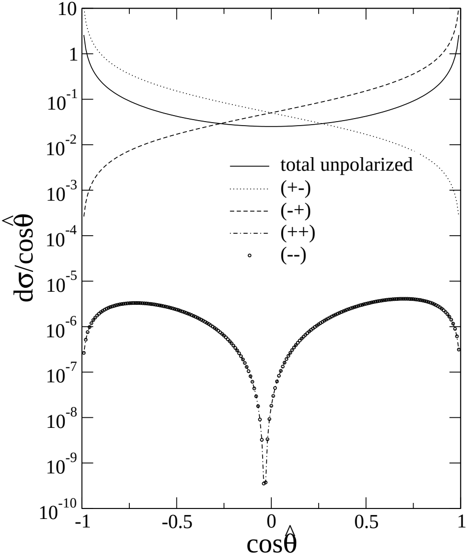

- $\mathcal{M}^{(+,-)}$ peaked in the backward direction $\mathcal{M}^{(-,+)}$ peaked in the forward direction $(J_z = \pm 2)$
- Dominance of diagrams with exchange of a massless lepton in t and u channel
- M^{++} and M^{--} $(J_z = 0)$ are suppressed !

Monochromatic angular distributions

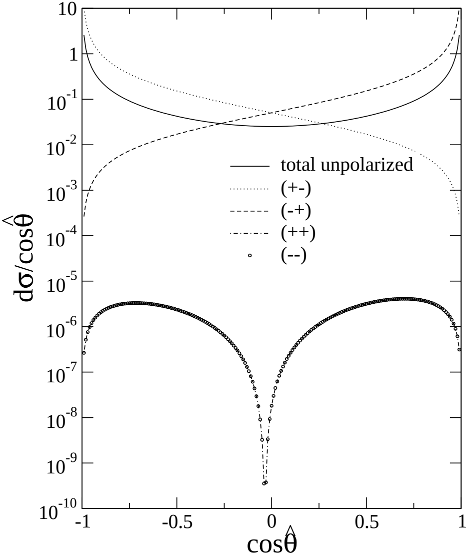

- $\mathcal{M}^{(+,-)}$ peaked in the backward direction $\mathcal{M}^{(-,+)}$ peaked in the forward direction $(J_z = \pm 2)$
- Dominance of diagrams with exchange of a massless lepton in t and u channel
- M^{++} and M^{--} $(J_z = 0)$ are suppressed !

The values of the masses are: $M_1 = 200$, $M_2 = 100$, $\langle \widetilde{m}_\ell \rangle = 150$ GeV, $\Delta m^2 = 6000$ GeV^2, $\sqrt{s_{\gamma\gamma}} = 128$ GeV

Monochromatic total cross-sections

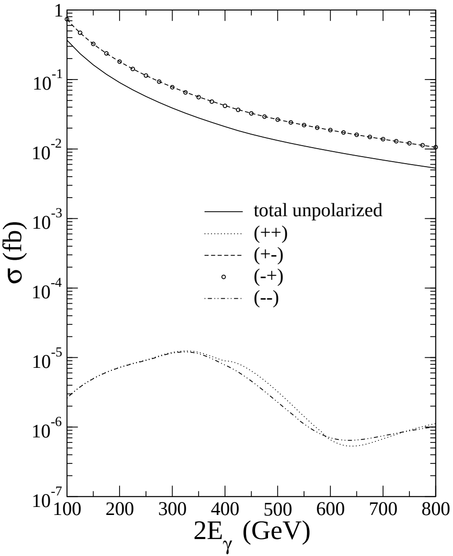

- Configurations with opposite helicity photons $\sigma_{(+,-)}$ and $\sigma_{(-,+)}$ ($J_z = \pm 2$) in the initial state dominate the signal.

Monochromatic total cross-sections

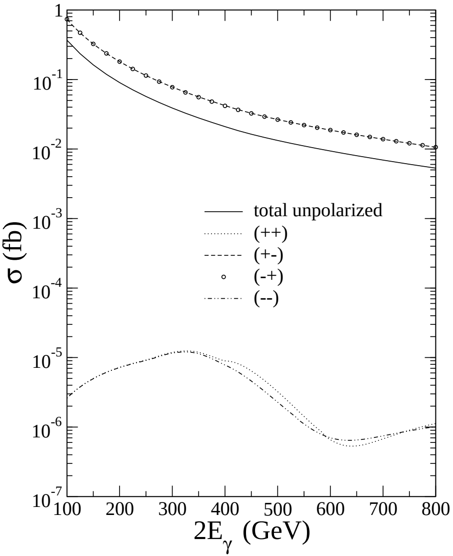

- Configurations with opposite helicity photons $\sigma_{(+,-)}$ and $\sigma_{(-,+)}$ $(J_z = \pm 2)$ in the initial state dominate the signal.
- Those with same helicity photons $(J_z = 0)$ give a negligible cross sections

Monochromatic total cross-sections

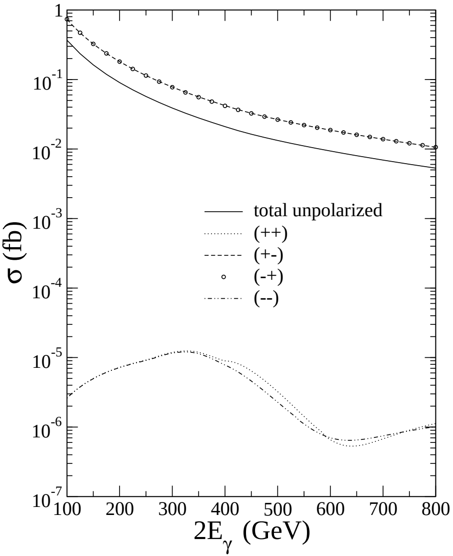

- Configurations with opposite helicity photons $\sigma_{(+,-)}$ and $\sigma_{(-,+)}$ $(J_z = \pm 2)$ in the initial state dominate the signal.
- Those with same helicity photons $(J_z = 0)$ give a negligible cross sections
- Signal cross section decreases with energy!

Monochromatic total cross-sections

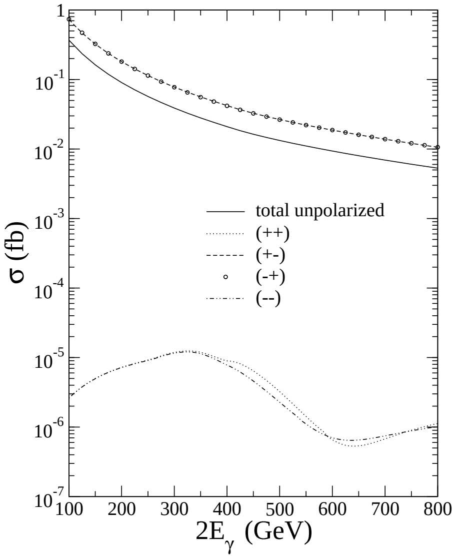

- Configurations with opposite helicity photons $\sigma_{(+,-)}$ and $\sigma_{(-,+)}$ $(J_z = \pm 2)$ in the initial state dominate the signal.
- Those with same helicity photons $(J_z = 0)$ give a negligible cross sections
- Signal cross section decreases with energy!

The values of the masses are: $M_1 = 200$, $M_2 = 100$, $\langle \widetilde{m}_\ell \rangle = 150$ GeV, $\Delta m^2 = 6000$ GeV^2.

Effect of spectra (angular distributions)

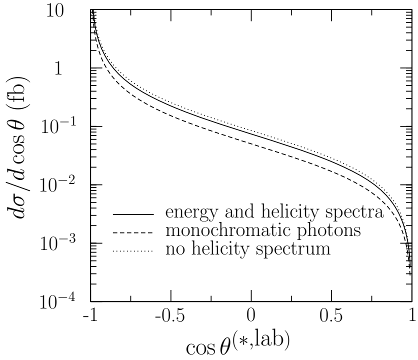

- Deviations from the complete formula depend on the angle; $\Rightarrow$less important where the angular distribution is largest.

Total cross section as a function of the LFV parametr δ_{LL}. The values of the masses are: $M_1 = 200$, $M_2 = 100$, $\langle \widetilde{m}_\ell \rangle = 150$ GeV, $\Delta m^2 = 6000$ GeV^2, $\sqrt{s_{\gamma\gamma}} = 128$ GeV.

Effect of spectra (angular distributions)

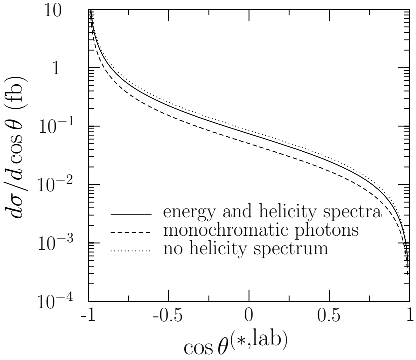

- Deviations from the complete formula depend on the angle; $\Rightarrow$less important where the angular distribution is largest.
- The effect of the helicity spectra is less important;

Total cross section as a function of the LFV parametr δ_{LL}. The values of the masses are: $M_1 = 200$, $M_2 = 100$, $\langle \widetilde{m}_\ell \rangle = 150$ GeV, $\Delta m^2 = 6000\ \text{GeV}^2$, $\sqrt{s_{\gamma\gamma}} = 128$ GeV.

Effect of spectra (total cross-sections)

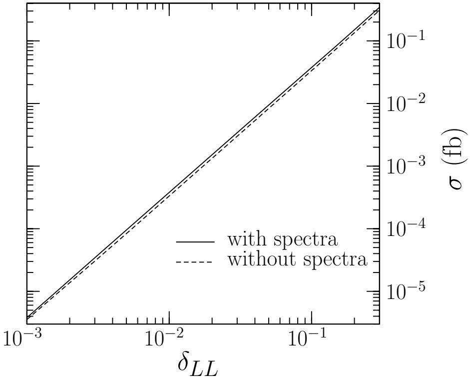

Effect of spectra (total cross-sections)

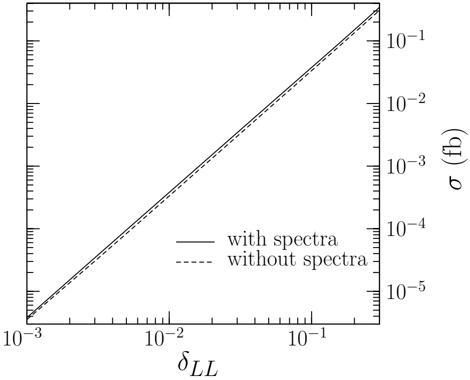

Total cross section as a function of the LFV parametr δ_{LL}. The values of the masses are: $M_1 = 200$, $M_2 = 100$, $\langle \widetilde{m}_\ell \rangle = 150$ GeV, $\Delta m^2 = 6000$ GeV^2, $\sqrt{s_{\gamma\gamma}} = 128$ GeV.

Effect of spectra (total cross-sections)

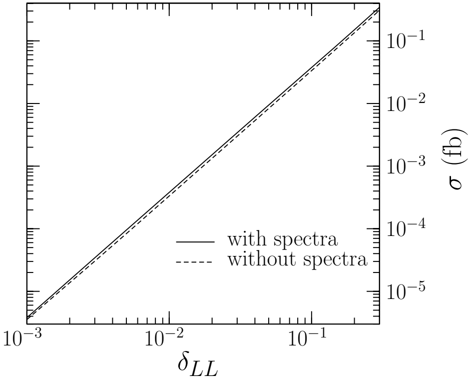

- Solid: with spectra; Dashed: monochromatic;

Total cross section as a function of the LFV parametr δ_{LL}. The values of the masses are: $M_1 = 200$, $M_2 = 100$, $\langle \widetilde{m}_\ell \rangle = 150$ GeV, $\Delta m^2 = 6000$ GeV^2, $\sqrt{s_{\gamma\gamma}} = 128$ GeV.

Effect of spectra (total cross-sections)

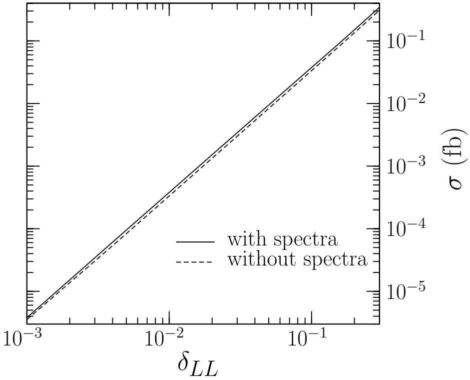

- Solid: with spectra; Dashed: monochromatic;
- The complete formula agrees within a few % with the monochromatic calculation with $E_\gamma = (E_\gamma)_{max}$

Total cross section as a function of the LFV parametr δ_{LL}. The values of the masses are: $M_1 = 200$, $M_2 = 100$, $\langle \widetilde{m}_\ell \rangle = 150$ GeV, $\Delta m^2 = 6000$ GeV^2, $\sqrt{s_{\gamma\gamma}} = 128$ GeV.

Scan of the SUSY parameter space $(\widetilde{m}, \delta_{LL})$: $\sqrt{s}_{\gamma\gamma} = 128\text{GeV}$, $\sqrt{s}_{ee} = 200\text{GeV}$, $L_{\gamma\gamma} = 136$ fb^{-1} yr^{-1}

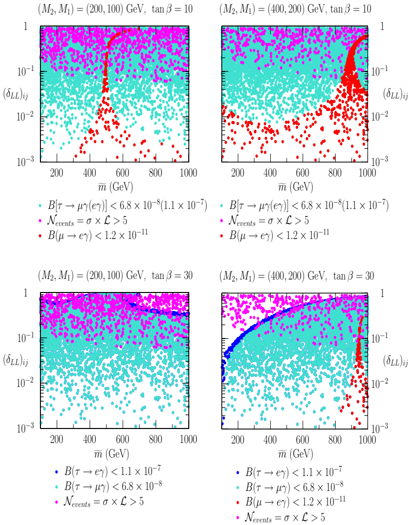

- $\widetilde{m}$ and $\delta_{LL} = \Delta m^2/\widetilde{m}^2$ are varied freely, for fixed value of gaugino masses;
- Cyan region ($\approx$ whole plane) is allowed by $Br(\tau \to \mu\gamma) < 6.8 \times 10^{-8}$ $Br(\tau \to e\gamma) < 3.9 \times 10^{-7}$
- Red region is allowed by $Br(\mu \to e\gamma) < 1.2 \times 10^{-11}$
- magenta region is where a PC can provide a positive signal of LFV: $N_{events} = L_{\gamma\gamma} \times \sigma_{signal} > 5$

The $(e\mu)$ channel is essentially excluded by the non observation of the $\mu \to e\gamma$ decay. LFV observable only in the $e\tau$ or $(\mu\tau)$ channels.

Standard Model Background

- Production of charged leptons will be copious in $\gamma\gamma$ collisions, and the SM provides several background processes:

$$
\begin{aligned}
&(a)\ \ \gamma\gamma \to \tau^-\tau^+ \to \tau^-\nu_e\bar{\nu}_\tau e^+ \\
&(b)\ \ \gamma\gamma \to W^{-*}W^{+*} \to \tau^-\bar{\nu}_\tau\, e^+\nu_e \\
&(c)\ \ \gamma\gamma \to e^+e^-\tau^+\tau^-
\end{aligned}
$$

with similar processes for the production of $\mu\tau$ pairs.

Standard Model Background

- Production of charged leptons will be copious in $\gamma\gamma$ collisions, and the SM provides several background processes:

$$\begin{aligned} (a)\ \ & \gamma\gamma \to \tau^-\tau^+ \to \tau^-\nu_e\bar{\nu}_\tau e^+ \\ (b)\ \ & \gamma\gamma \to W^{-*}W^{+*} \to \tau^-\bar{\nu}_\tau\, e^+\nu_e \\ (c)\ \ & \gamma\gamma \to e^+e^-\tau^+\tau^- \end{aligned}$$

with similar processes for the production of $\mu\tau$ pairs.

- The $e\mu$ final state, (which from the experimental point of view is the easiest to reconstruct), is almost completely excluded by the strong bounds from the non observation of the radiative decay $\mu \to e\gamma$.

Standard Model Background

- Production of charged leptons will be copious in $\gamma\gamma$ collisions, and the SM provides several background processes:

$$
\begin{aligned}
(a)&\ \ \gamma\gamma \to \tau^-\tau^+ \to \tau^-\nu_e\bar{\nu}_\tau e^+ \\
(b)&\ \ \gamma\gamma \to W^{-*}W^{+*} \to \tau^-\bar{\nu}_\tau\, e^+\nu_e \\
(c)&\ \ \gamma\gamma \to e^+e^-\tau^+\tau^-
\end{aligned}
$$

  with similar processes for the production of $\mu\tau$ pairs.
- The $e\mu$ final state, (which from the experimental point of view is the easiest to reconstruct), is almost completely excluded by the strong bounds from the non observation of the radiative decay $\mu \to e\gamma$.
- Thus we are bound to consider signals with τ's in the final state.

Applied kinematical cuts

- The signal has two back-to-back leptons *without missing transverse momentum and energy.*

Applied kinematical cuts

- The signal has two back-to-back leptons *without missing transverse momentum and energy.*
- The angular cut $|\cos(\theta)| < 0.9$ ($\theta < 25.8°$) applied to the signal is also applied to the background.

Applied kinematical cuts

- The signal has two back-to-back leptons *without missing transverse momentum and energy*.
- The angular cut $|\cos(\theta)| < 0.9$ ($\theta < 25.8^\circ$) applied to the signal is also applied to the background.
- We impose the back-to-back condition on the background processes requiring $180^\circ - \theta_{\ell\ell'} < 5^\circ$.

Applied kinematical cuts

- The signal has two back-to-back leptons *without missing transverse momentum and energy.*
- The angular cut $|\cos(\theta)| < 0.9$ ($\theta < 25.8^\circ$) applied to the signal is also applied to the background.
- We impose the back-to-back condition on the background processes requiring $180^\circ - \theta_{\ell\ell'} < 5^\circ$.
- Leptons are required to have energy close to E_γ, at least 85% of the maximum photons energy $E^\gamma_{max} = y_{max} E_0$.

SM Background

Total cross section without (above) and with cuts (below) for the background processes.

$2E_0$ (GeV)	$\gamma\gamma \to \tau\tau \to \tau e\nu\bar{\nu}$	$\gamma\gamma \to WW \to e\tau\nu\bar{\nu}$	$\gamma\gamma \to \tau\tau ee$
200	0.58 fb 1.49×10^{-6} fb	2.3×10^{-1} //	36.7 pb 4.4×10^{-2} fb
300	3.1 fb 16.3×10^{-6} fb	0.48 pb //	38.9 pb 3.7×10^{-2} fb
400	4.9 fb 3.9×10^{-4} fb	0.69 pb 2.1×10^{-2}	39.5 pb 2.9×10^{-2} fb
500	6.1 fb 9.7×10^{-4} fb	0.77 pb 1.0×10^{-1}	39.9 pb 2.4×10^{-2} fb

The configuration that mimics the signal arises if one $e\tau$ pair is emitted at small angles along the collision axis and *is not* detected (we require $\theta_\ell^{untagged} < 25.8°$), while the other pair is tagged. After cuts the cross section is effectively reduced by orders of magnitudes, it is still at the level of 10^{-2} fb.

Statistical Significance

- However as a final step the SM background can be estimated requiring instead that the detected τ and electron be of the *same* charge, and eventually it could be subtracted.

Statistical Significance

- However as a final step the SM background can be estimated requiring instead that the detected τ and electron be of the *same* charge, and eventually it could be subtracted.
- Finally consider the statistical significance (SS) and require:

$$SS = \frac{\mathcal{L}\sigma_{cut}^{Sig}}{\sqrt{\mathcal{L}\sigma_{cut}^{BG}}} \geq 3$$

This implies (with simulated annual luminosity for TESLA):

$$\sqrt{s_{ee}} = 200\,\text{GeV} \Rightarrow \sigma_{cut}^{Sig} > 5.4 \times 10^{-2}\,\text{fb} \Rightarrow \delta_{LL} \gtrsim 10^{-1}$$
$$\sqrt{s_{ee}} = 500\,\text{GeV} \Rightarrow \sigma_{cut}^{Sig} > 2.5 \times 10^{-2}\text{fb} \Rightarrow \delta_{LL} \gtrsim 10^{-1}$$

Outline

1. Introduction
2. SUSY scenario for Lepton Flavor Violation
3. Cross sections at a Photon Collider and Backgrounds
   - Photon Beams
   - Signal Cross sections
   - Standard Model Background
4. Summary
   - Conclusions

Conclusions

- We have studied the LFV reactions $\gamma\gamma \to \ell\ell'$ ($\ell, \ell' = e, \mu, \tau$, $\ell \neq \ell'$) which arise at the one loop order of perturbation theory of interest for the $\gamma\gamma$ option of the future ILC.

Conclusions

- We have studied the LFV reactions $\gamma\gamma \to \ell\ell'$ ($\ell, \ell' = e, \mu, \tau$, $\ell \neq \ell'$) which arise at the one loop order of perturbation theory of interest for the $\gamma\gamma$ option of the future ILC.
- The LFV mechanism is provided by non diagonal entries of the charged slepton mass matrices ascribed

Conclusions

- We have studied the LFV reactions $\gamma\gamma \to \ell\ell'$ ($\ell, \ell' = e, \mu, \tau$, $\ell \neq \ell'$) which arise at the one loop order of perturbation theory of interest for the $\gamma\gamma$ option of the future ILC.
- The LFV mechanism is provided by non diagonal entries of the charged slepton mass matrices ascribed
- We have studied the signal in a model independent way in order to pin down regions of the SUSY parameter space $(\widetilde{m}_\ell, \delta_{LL})$ plane, allowed by the present experimental limits.

Conclusions

1. In the range $\sqrt{s_{ee}} \approx 200 - 500$ GeV the cross section of the signal is $\sigma(\gamma\gamma \to \ell\ell') \approx \mathcal{O}(10^{-1} - 10^{-2})$ fb, (sparticle masses $\approx 100 - 400$ GeV) i.e. a light SUSY spectrum somehow hinted to by fits on standard model parameters and SUSY benchmark points.

Conclusions

1. In the range $\sqrt{s_{ee}} \approx 200 - 500$ GeV the cross section of the signal is $\sigma(\gamma\gamma \to \ell\ell') \approx \mathcal{O}(10^{-1} - 10^{-2})$ fb, (sparticle masses $\approx 100 - 400$ GeV) i.e. a light SUSY spectrum somehow hinted to by fits on standard model parameters and SUSY benchmark points.
2. Observation of $\gamma\gamma \to e\tau$, $(\mu\tau)$ is not excluded by present bounds on the radiative lepton decays $\tau \to e\gamma$, $\tau \to \mu\gamma$. However a $\delta_{LL} = \Delta m^2/\widetilde{m}_\ell^2 \approx \mathcal{O}(10^{-1})$ is required, (possible only within some specific models of the SUSY see-saw framework).

Conclusions

1. In the range $\sqrt{s_{ee}} \approx 200 - 500$ GeV the cross section of the signal is $\sigma(\gamma\gamma \to \ell\ell') \approx \mathcal{O}(10^{-1} - 10^{-2})$ fb, (sparticle masses $\approx 100 - 400$ GeV) i.e. a light SUSY spectrum somehow hinted to by fits on standard model parameters and SUSY benchmark points.
2. Observation of $\gamma\gamma \to e\tau$, $(\mu\tau)$ is not excluded by present bounds on the radiative lepton decays $\tau \to e\gamma$, $\tau \to \mu\gamma$. However a $\delta_{LL} = \Delta m^2/\widetilde{m}_\ell^2 \approx \mathcal{O}(10^{-1})$ is required, (possible only within some specific models of the SUSY see-saw framework).
3. The $e\mu$ final state is almost excluded by $Br(\mu \to e\gamma) \leq 1.2 \times 10^{-11}$, four orders of magnitude smaller than $Br(\tau \to e\gamma)$, $Br(\tau \to \mu\gamma)$.

Conclusions

1. In the range $\sqrt{s_{ee}} \approx 200 - 500$ GeV the cross section of the signal is $\sigma(\gamma\gamma \to \ell\ell') \approx \mathcal{O}(10^{-1} - 10^{-2})$ fb, (sparticle masses $\approx 100 - 400$ GeV) i.e. a light SUSY spectrum somehow hinted to by fits on standard model parameters and SUSY benchmark points.
2. Observation of $\gamma\gamma \to e\tau$, $(\mu\tau)$ is not excluded by present bounds on the radiative lepton decays $\tau \to e\gamma$, $\tau \to \mu\gamma$. However a $\delta_{LL} = \Delta m^2/\widetilde{m}_\ell^2 \approx \mathcal{O}(10^{-1})$ is required, (possible only within some specific models of the SUSY see-saw framework).
3. The $e\mu$ final state is almost excluded by $Br(\mu \to e\gamma) \leq 1.2 \times 10^{-11}$, four orders of magnitude smaller than $Br(\tau \to e\gamma)$, $Br(\tau \to \mu\gamma)$.
4. The SM process $\gamma\gamma \to ee(\mu\mu)\tau\tau$ with an undetected $e\tau$ pair is potentially large. It can be reduced at the level of $\sigma_{back} \approx \mathcal{O}(10^{-2})$ fb.
   However $SS \gtrsim 3$ provided that $\delta_{LL} \gtrsim 10^{-1}$.